

Figure 1. Generalized surface geology map of Sabine Peninsula (after Harrison, 1994) displaying sedimentary stratigraphic divisions.

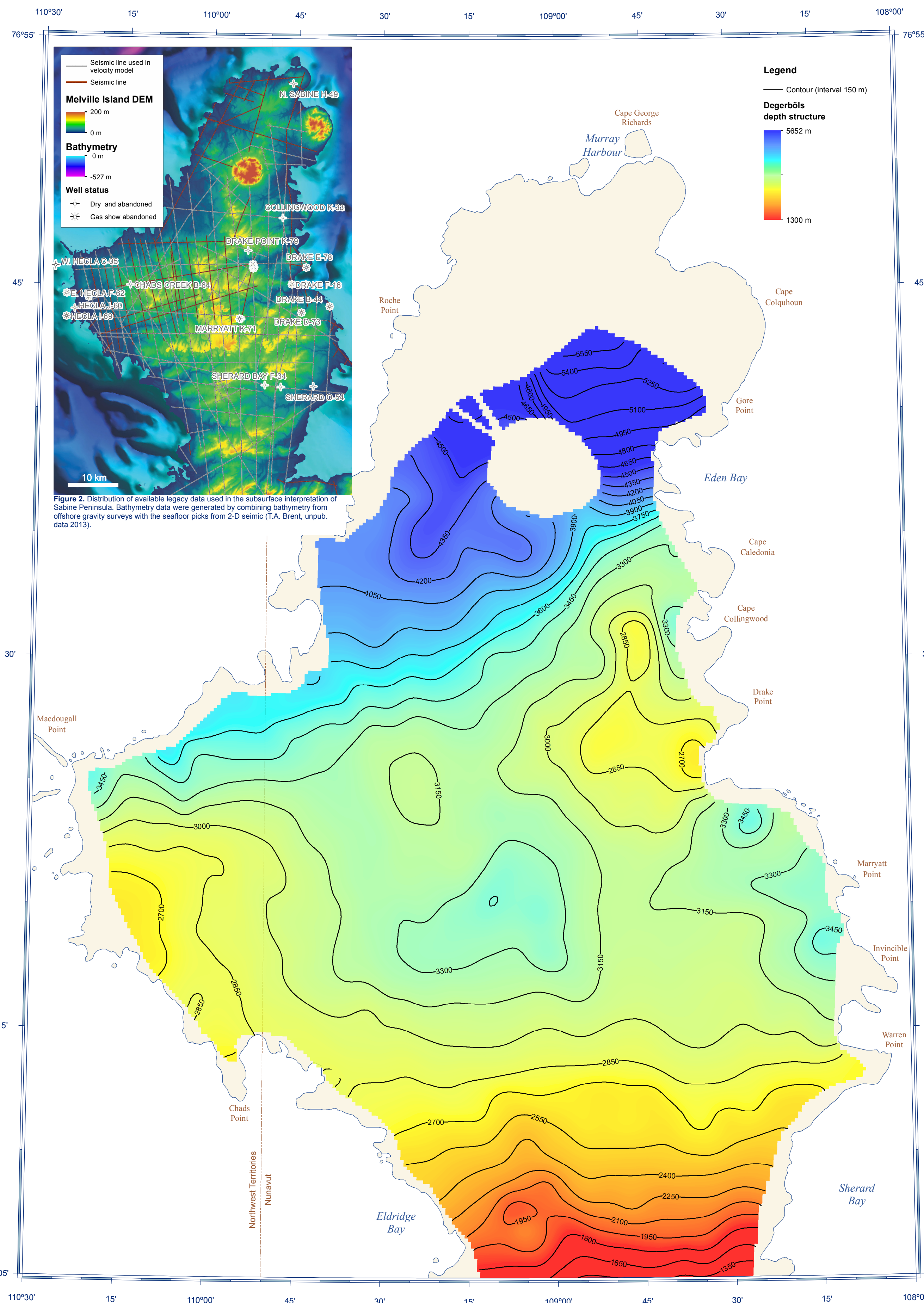


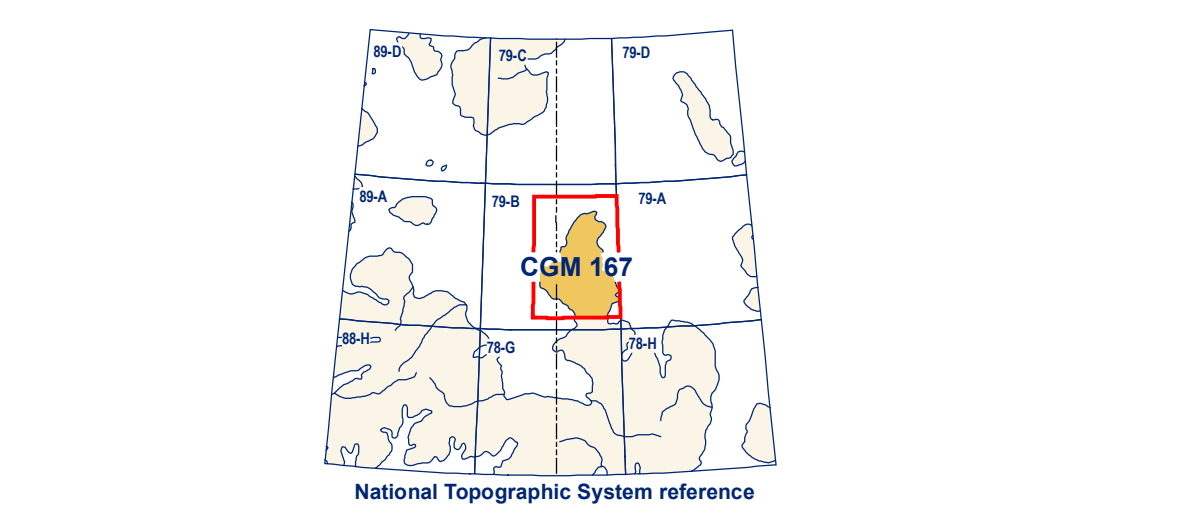
Figure 2. Distribution of available legacy data used in the subsurface interpretation of Sabine Peninsula. Bathymetry data were generated by combining bathymetry from offshore gravity surveys with the seafloor picks from 2-D seismic (T.A. Brent, unpub. data 2013).

**Abstract**  
Sabine Peninsula of Melville Island was the subject of an oil and gas exploration boom from 1981 to 1985, during which time seismic-reflection data were collected and wells were drilled. As a result, the two largest conventional natural gas fields in Canada were discovered.

**Résumé**  
La péninsule de Sabine de l'île de Melville a connu un boom d'exploration pétrolière et gazière entre 1981-1985 pendant lequel des données de sismique-réflexion furent acquises et des puits forés. Les résultats les plus importants ont été la découverte de deux plus grands champs de gaz naturel conventionnels du Canada.

Seismic-reflection methods use sound waves to image the internal structure of the Earth. Waves are emitted at the surface before being reflected back to the surface by geological interfaces and recorded. Modern analysis methods were used to re-investigate existing seismic data. In doing so, eight seismic unit boundaries identified on seismic profiles in two-way time were correlated to the regional geological framework and gridded to provide subsurface maps. Each map approximates the geological knowledge at that particular time or depth allowing the enhancement of the geological knowledge of Sabine Peninsula and better delineation of elements of the petroleum systems therein.

La sismique-réflexion utilise des ondes sonores pour imaginer la structure interne de la Terre. Les ondes sont émises au surface avant d'être réfléchies et de nouveau vers la surface par des interfaces géologiques et elles sont enregistrées. Des méthodes d'analyse modernes furent utilisées pour ré-investiger des données sismiques existantes. Ainsi, huit limites d'unités sismiques identifiées sur les profils sismiques en temps de parcours aller-retour furent corrélées au cadre géologique régional et maillées afin de produire des cartes de la sous-surface. Chaque carte est une approximation des connaissances géologiques à un certain temps ou une certaine profondeur nous permettant d'améliorer nos connaissances géologiques de la péninsule de Sabine et de mieux délimiter les éléments des systèmes pétroliers s'y trouvant.



**Cover Illustration**  
Permian sandstone hoodoos, Sabine Peninsula, Melville Island, Nunavut. Photograph by T.A. Brent, 2013-242

Catalogue No. M163-1167-2013E-PDF  
ISBN 978-1-100-29292-5  
doi:10.4095/293091

© Her Majesty the Queen in Right of Canada 2013

**Canada** Natural Resources Canada / Ressources naturelles du Canada

**CANADIAN GEOSCIENCE MAP 167**  
**TIME- AND DEPTH-STRUCTURE MAP**  
**DEGERBÖLS FORMATION**

Sabine Peninsula, Melville Island  
Nunavut-Northwest Territories  
1:200 000

**TIME- AND DEPTH-STRUCTURE MAP**  
**DEGERBÖLS FORMATION**  
Sabine Peninsula, Melville Island  
Nunavut-Northwest Territories  
1:200 000

Authors: M.J. Duchesne, V.I. Brake, K. Dawing, M. Claproot, E. Gloaguen, and T.A. Brent  
Time-structure map by V.I. Brake and M.J. Duchesne, Geological Survey of Canada, 2013  
Depth-structure map by M.J. Duchesne and V.I. Brake, Geological Survey of Canada, 2013  
Seismic interpretation by V.I. Brake, M.J. Duchesne, Geological Survey of Canada, 2010-2013

Geomatics by V.I. Brake, Geological Survey of Canada and G. Huot-Vézina, Institut national de la recherche scientifique  
Cartography by R. Boivin  
Scientific editing by E. Inglis  
Initiative of the Geological Survey of Canada, conducted under the auspices of the Western Arctic Islands project as part of Natural Resources Canada's Geo-mapping for Energy and Minerals (GEM) program.

Map projection Universal Transverse Mercator, zone 12  
Base map at the scale of 1:250 000 from Natural Resource Canada, with modifications.  
Proximity to the North Magnetic Pole causes the magnetic compass to be useless in this area.  
This map is not to be used for navigational purposes.

The Geological Survey of Canada welcomes corrections or additional information.  
The data may include additional observations not portrayed on this map. See documentation accompanying the data.  
This publication is available for free download through GEOCAN (http://geocan.ess.nrcan.gc.ca/).  
This map is not to be used for navigational purposes.

**DESCRIPTIVE NOTES**

**INTRODUCTION**  
The time- and depth-structure maps presented herein are part of an eight-map series of the subsurface of Sabine Peninsula spanning the Early Permian through Early Cretaceous interval. These maps are the product of the application of modern geoscientific methods of processing and interpretation to a suite of legacy seismic-reflection data from onshore Sabine Peninsula (Melville Island, Western Arctic Islands). The resulting processed seismic lines were interpreted using the existing regional geological framework (see Harrison, 1999) by integrating existing regional well data, geophysical logs, age control, and lithological information through synthetic seismograms.

**REGIONAL SETTING**  
The Sabine Peninsula of Melville Island is located within the Sverdrup Basin in the Queen Elizabeth Islands of the western Arctic. The Sverdrup Basin extends for about 1300 km in a northeast-southwest direction and is up to 350 km wide. The basin contains up to 13 km of sedimentary strata (Embry and Beauchamp, 2008). The Sverdrup Basin is separated from the underlying Franklin Basin by an unconformity at the base of the Carboniferous strata. The Franklin Basin was deposited by widespread fluvial-lacustrine Carboniferous-Early Permian Orogeny. The resulting rift-related structural depression acted as a major depocentre from the Carboniferous through the Paleogene (Embry and Beauchamp, 2008). The Sverdrup Basin succession was uplifted and deformed during the Cenozoic-Eurasian Orogeny.

The surface geology of Melville Island is dominated by Lower Paleozoic strata of the Franklin Basin. The Sabine Peninsula is an exception to this, as surface strata are part of the Sverdrup Basin. The geology of the Sabine Peninsula consists of deformed Late Carboniferous to Paleocene sandstone, siltstone, shale, and minor amounts of carbonate. Additionally, evaporitic rocks are exposed in two diapirs on northern Sabine Peninsula—the Barrow and Colquhoun domes, which consist of deformed anhydrite and gypsum. The strata of the Sverdrup Basin succession on the northern part of the peninsula and the Drake Point anticline and the Maryatt Point syncline to the south (Harrison, 1994) (Fig. 1).

During a 1981 to 1985 phase of petroleum exploration, companies drilled 52 wells on Melville Island and surrounding waters (22 of which were on Sabine Peninsula) and acquired about 3,400 line-kilometres of onshore seismic-reflection data (Fig. 2). Three separate gas fields were discovered in the Sabine Peninsula area: Drake Point, Hecla, and Roche Point. Feasibility studies for the development of the gas fields were conducted in the early 1980s; however, due to low gas prices and the lack of gas markets, the gas fields on Melville Island (and elsewhere in the Canadian Arctic) were not developed (Harrison, 1995).

**SEISMIC DATA SET AND PROCESSING**  
Data access was obtained through a Memorandum of Understanding signed in 1997 by the Geological Survey of Canada (GSC), Panarctic Oils, the Arctic Islands Exploration Group, and the Offshore Arctic Exploration Group venture parties. The data sets consist of original land seismic-reflection field tapes transcribed from 21-, 7-, and 9-track media. Data were collected using a dynamic charge of 20–30 kg per shot at about 20 m below the surface. Shot-point spacing ranged from 60 m to 300 m, the shorter spacing being used for most surveys. The majority of the seismic-reflection data were recorded using 48- or 96-channel systems. Channels were generally deployed using line receivers spaced at about 8 m and station intervals varying from 50 m to 70 m. The common-midpoint multiplicity of the data sets range from 1 to 12-fold coverage. The most common recording length was 6 s.

The processing consisted of three main steps: 1) principal component decomposition was used to remove both coherent and random noise; 2) data were migrated utilizing poststack Kirchhoff migration; and 3) seismic sandstones were extended to increase vertical resolution (Claproot et al., 2011; Duchesne et al., 2012).

**Velocity model**  
A 3-D velocity model was built using about 1300 km of linear seismic data (70 lines) and 13 wells spread over an area of about 2800 km<sup>2</sup> (Fig. 2). The velocity model was then used for poststack migration processing and to convert seismic horizon surfaces from time to depth. The primary assumption behind the velocity model is that the coherent high-amplitude reflections that were picked to build the model correspond to important acoustic impedance contrasts caused by significant and abrupt velocity changes. This assumption was confirmed by tying seismic picks to well sonic logs (Duchesne et al., 2012). The geostatistical approach of kriging with an external drift (KED) was applied to both the reflection time of the picked seismic horizons and time-depth pairs derived from check shot data to compute the 3-D velocity field. Kriging interpolates values between known positions based on weighted spatial correlations. The KED technique was specifically developed for the integration of seismic data into the kriging process where the number of wells is insufficient for the computation of adequate depth statistics (Haas and Dubrule, 1994). Hence, it uses the information provided by the time horizon picks to improve estimates where depth control is sparse. For seismic migration, root-mean squared (RMS) velocity values are first estimated by KED from time-to-depth conversion of seismic horizon surfaces mapped as important velocity boundaries (Duchesne et al., 2012). Then, once the approximate depths of the surfaces are known, the interval velocities ( $V_{int}$ ) for all time intervals delimited by two consecutive horizons are computed from:

$$V_{int} = \frac{\Delta z}{\Delta t_i}$$

where  $\Delta z$  and  $\Delta t_i$  are the depth and time intervals between two successive horizons  $i$ . Once  $V_{int}$  is obtained the RMS velocity ( $V_{rms}$ ) is calculated using:

$$V_{rms} = \sqrt{\frac{1}{N} \sum_{i=1}^N V_{int}^2 \Delta t_i}$$

in which  $N$  is the total number of horizons and  $\Delta t_i$  is the sum of all time intervals.

**SEISMIC INTERPRETATION AND VISUALIZATION METHODS**  
Processed seismic lines were loaded into IHS-Kingdom 2D seismic and geological interpretation software. Prominent seismic-reflection horizons, tied to well formation-top information, were manually correlated. Seed points were generated at seismic line intersections, thereby permitting the interpretation of anticlines.

The map would benefit from a detailed structural interpretation; however, confidence of this interpretation is minimized due to minor vertical offsets (about 0.1 s) attributed to faulting and the large line spacing. Thus, reflections are readily identified across faults despite offset.

Time-structure maps of the key seismic horizons were computed using universal kriging. Universal kriging permits the interpolation of a nonstationary random field by adding a term in the kriging equation that accommodates any linear trends present in a scattered point set (Chiles and Delhomme, 1999). Given that all picked horizons showed a strong linear trend for time versus depth over distance, universal kriging provided the best fit to the picked horizons.

**TIME TO DEPTH CONVERSION**  
All time surfaces are converted to depth using the following procedure. First  $V_{int}$  of the 3-D velocity model are calculated using the Dix equation:

$$V_{int} = \left[ \frac{V_{i+1}^2 - V_i^2}{t_{i+1} - t_i} \right]^{1/2}$$

where  $t$  is the zero-offset arrival time of the  $i$ th reflection. Interval limits corresponded to seismic horizons that are picked and tied to geological interfaces. Then  $V_{int}$  are extracted from the velocity model along picked horizons. Velocity maps are then computed using Universal kriging at a cell size of 250 m. Finally, the time-structure surfaces of the various seismic horizons are converted to depth ( $Z$ ) using:

$$Z = \frac{t_{int} \cdot V_{int}}{2}$$

Because the depth conversion process is a function of the velocity model, the lateral extent of depth maps is confined to the lateral extent of the model. The final depth-structure maps were imported into ArcGIS for visualization using the Arc extension Team-GIS Bridge.

**UNCERTAINTY**

Quantifying the uncertainty of seismic subsurface maps is difficult since several sources of data, each with their unique level of uncertainty, are used in the map generation. Sources of error may arise from limitations in acquisition, processing, and interpretation. Moreover, seismic data are collected remotely and the images they provide are derived from generalized mathematical and physical concepts. Constraints on acquisition that increase the uncertainty include gaps in coverage because of obstacles to source and receiver deployment, and effect of direction of shooting on data quality (Sherrill and Geldart, 1995). Processing errors may result from inadequate static corrections, inaccurate velocity analysis, and inappropriate parameter determination.

More specifically to this data set, errors may have also been introduced by the velocity model and the ability to form top to seismic horizons. The velocity model represents an estimation of the velocity fluctuations for which the accuracy depends on the number of wells and the good fit between time picks and corresponding depths at the well locations. A regression analysis shows that time picks and their corresponding depths at the wells have a strong linear fit ( $r^2 = 0.98$ ), meaning that the use of time picks as the external drift in the kriging strategy is justified and accurate. Nevertheless, the uncertainty of the velocity model increases when the distance between the well and any points where velocity is predicted exceeds the range of the variogram used. In the present case, the uncertainty between depth and time increases when the range of different horizons is between 5 km and 34 km. The ability to form top to seismic horizons relies on the successful use of well sonic and density logs, since it is the contrast between the product of these properties for two successive geological layers that generates reflections recorded in seismic exploration. Formation tops used in this study are from Dawing and Embry (2007), for which they mainly utilized gamma-ray logs to position the upper limit of the formations in depth. Thus errors may have been introduced by projecting the formation tops on seismic sections recorded in time.

**TIME- AND DEPTH-STRUCTURE DATA DISPLAY**  
The time- and depth-structure data shown on this map were gridded at a cell size of 250 m using Universal kriging. Each map presents a grid with a stretched colour ramp at 20% transparency. Time contours generated from the time-structure grids are shown in black at 100 ms interval, whereas depth contours derived from the depth-structure grid are presented at 150 m intervals.

**DEGERBÖLS MAP DESCRIPTIONS**

The Middle Permian Degerböls Formation consists of bioturbated and locally fossiliferous carbonate and is laterally equivalent to shale, chert, carbonate, and diolomitoclasts of the Middle Permian van Hauen Formation. The formation-top data indicates interfingering between the Degerböls and van Hauen formations, occasionally interrupted by intrusive dykes and sills (Dewing and Embry, 2007, see also Fig. 3). The Degerböls Formation is herein defined to include the laterally equivalent van Hauen Formation. The combination of interfingering and the intrusions makes the thickness difficult to estimate.

The mapped Degerböls Formation reflection extends from the narrowest point of the peninsula near Eldridge and Sheppard bays to near the axis of the Murray Harbour syncline. The data gap west of Eden Bay marks the location of Barrow Dome. Two-way traveltimes increase northward from 750 ms to 3275 ms, or from 1300 m to 5627 m. The slope of the Degerböls Formation horizon generally falls between 0.5° and 4.5°, however, steeper slopes up to 10° are observed at the northern and southern ends of the peninsula. The surface dips into a distinctive depression at the centre of Sabine Peninsula. It is delimited by the Drake Point anticline to the north and the Maryatt Point syncline to the south (Harrison, 1994).

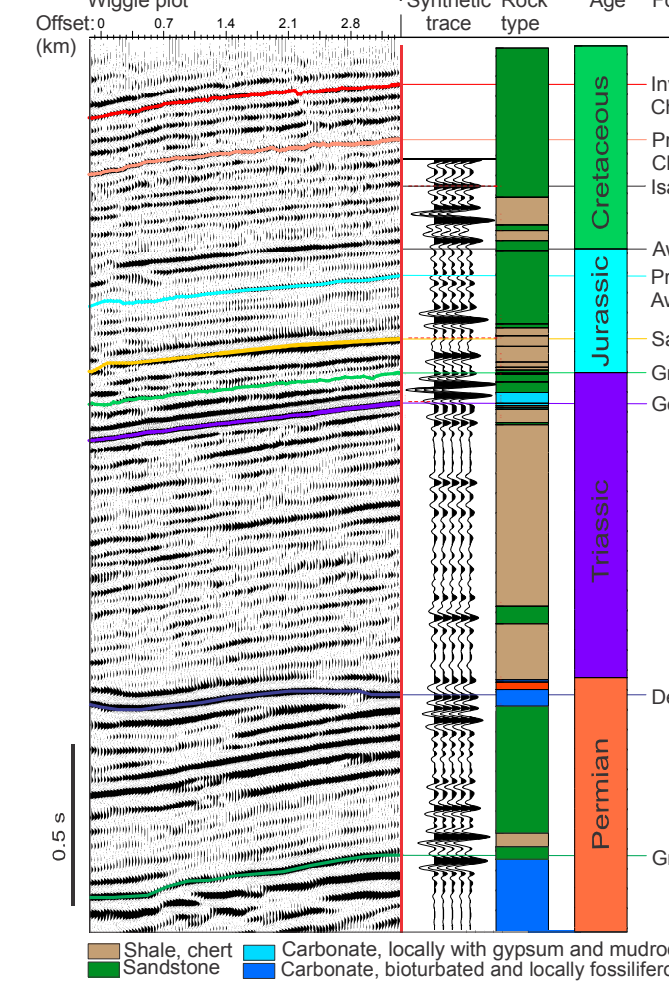


Figure 3. Comparison of the wiggle plot, synthetic trace, stratigraphy, age, and formation-top data for the Chads Creek B-64 well.

**ACKNOWLEDGMENTS**

The authors would like to thank J. Dietrich and B. MacLean (GSC Calgary) for their technical review that improved the overall quality of the maps. IHS is acknowledged for providing Kingdom 8.8 seismic interpretation software.

**REFERENCES**

Chiles, J.P. and Delhomme, P., 1999. Geostatistics: Modeling Spatial Uncertainty. Wiley Series in Probability and Statistics. Wiley, New York, New York, 749 p.

Claproot, M., Duchesne, M.J., and Gloaguen, E., 2011. A geostatistical approach for 2-D seismic velocity modeling. Geological Survey of Canada, Open File 7045, 21 p. doi:10.4095/289551

Dewing, K. and Embry, A.F., 2007. Geophysical and geochemical data from the Canadian Arctic Islands. Part I: Stratigraphic tops from Arctic Islands. Oil and Gas Technology Journal, Geological Survey of Canada, Open File 5442, 110 p. doi:10.4095/223886

Duchesne, M.J., Claproot, M., and Gloaguen, E., 2012. Improving seismic velocity estimation for 2-D poststack time migration of regional seismic data using kriging with an external drift. The Leading Edge, v. 31, p. 1196-1198.

Embry, A. and Beauchamp, B., 2008. Sverdrup Basin: In Sedimentary Basins of the World, (ed. K.J. Hol), Volume 5, The Sedimentary Basins of the United States and Canada. Elsevier, Amsterdam, The Netherlands, p. 461-471.

Harrison, J.C., 1994. Melville Island and adjacent smaller islands, Canadian Arctic Archipelago, District of Franklin, Northwest Territories. Geological Survey of Canada, Map 1544A, scale 1:250 000. doi:10.4095/203577

Harrison, J.C., 1996. Melville Islands salt-based fold belt, Arctic Canada. Geological Survey of Canada, Bulletin 472, 344 p. doi:10.4095/203578

Haas, A. and Dubrule, O., 1994. Geostatistical inversion – a sequential method of stochastic reservoir modeling constrained by seismic data. First Break, v. 12, p. 551-559.

Sherrill, R.E. and Geldart, L.P., 1995. Exploration Seismology. Cambridge University Press, New York, New York, 628 p.

**Recommended citation**  
Duchesne, M.J., Brake, V.I., Dawing, K., Claproot, M., Gloaguen, E., and Brent, T.A., 2013. Time- and depth-structure map, Degerböls Formation, Sabine Peninsula, Melville Island, Nunavut-Northwest Territories. Geological Survey of Canada, Canadian Geoscience Map 167, scale 1:200 000. doi:10.4095/293091